NASA TECHNICAL MEMORANDUM 102728

A MACRO-MICROMECHANICS ANALYSIS OF A NOTCHED METAL MATRIX COMPOSITE

C. A. Bigelow and R. A. Naik

September 1990

National Aeronautics and
Space Administration

Langley Research Center
Hampton, Virginia 23665

SUMMARY

A macro-micromechanics analysis was formulated to determine the matrix and fiber behavior near the notch tip in a center-notched metal matrix composite. Results are presented for a boron/aluminum monolayer. The macro-level analysis models the entire notched specimen using a three-dimensional finite element program which uses the vanishing-fiber-diameter model to model the elastic-plastic behavior of the matrix and the elastic behavior of the fiber. The micro-behavior is analyzed using a discrete fiber-matrix (DFM) model containing one fiber and the surrounding matrix. The dimensions of the DFM model were determined by the ply thickness and the fiber volume fraction and corresponded to the size of the notch-tip element in the macro-level analysis. The boundary conditions applied to the DFM model were determined from the macro-level analysis. Stress components within the DFM model were calculated and stress distributions are presented along selected planes and surfaces within the DFM model, including the fiber-matrix interface. Yielding in the matrix was examined at the notch tip in both the macro- and micro-level analyses. The DFM model predicted higher stresses (24%) in the fiber compared to the global analysis. In the notch-tip element, the interface stresses indicated that a multi-axial stress criterion may be required to predict interfacial failure. The DFM analysis predicted yielding to initiate in the notch-tip element at a stress level 28% lower than predicted by the global analysis.

INTRODUCTION

Metal matrix composites have several inherent properties, such as high stiffness-to-weight ratios and high strength-to-weight ratios, which make them attractive for structural applications. These composites also have a higher operating temperature range and better environmental resistance than current polymer matrix composites. Like polymer matrix composites, however, metal matrix composites are notch sensitive. Unlike typical polymer matrix composites, metal matrix composites may exhibit wide spread yielding of the matrix before laminate failure. To design damage-tolerant structures (or to simply understand the effects of fastener holes), the laminate fracture strengths must be known for a wide range of ply orientations, notch geometries, and loading conditions. A method for predicting fracture strength is needed to avoid testing all the laminate, notch, and loading combinations of interest.

The present paper combines a three-dimensional homogeneous, orthotropic finite element analysis of a center-notched tension specimen and a discrete fiber-matrix micromechanics model of a single fiber. The displacements predicted by the macro-level analysis of the tensile specimen were imposed as boundary conditions on the discrete fiber-matrix (DFM) micro-model. To demonstrate this approach, results are presented for a single metal matrix composite, a boron/aluminum (B/Al) monolayer. Testing of this specimen was described in [1].

A global-local, or substructuring, approach has been used in the past for the analysis of complex structures, where the global analysis would address a large structure and the local analysis would analyze structural details, such as bolt holes (e.g., ref. 2). In the present work, a slightly different

approach is used in that the local analysis is a micromechanics analysis, analyzing a single fiber and its surrounding matrix as two discrete materials. Work has also been done using the "unit cell" micromechanical analysis, assuming an infinitely repeating array of fibers with the appropriate boundary conditions (see, for example, refs. 3-5). Square arrays, hexagonal arrays, and other configurations have been used. The present work uses the basic configuration of a unit cell, but in a slightly different manner. Instead of applying the boundary conditions corresponding to some assumed array of fibers and analyzing a unit cell representative of this array, the necessary displacement boundary conditions are obtained from the global or macro-level analysis of the notched specimen. By using these specific boundary conditions, the unit cell of fiber and matrix is in a stress state identical to that occurring in the macro-level analysis, thus, analyzing a unit cell at a specific location in a laminate. The approach used in this work will be referred to as a macro-micro analysis.

This approach, in effect, joins an element with discrete fiber and matrix to elements that are orthotropic but homogeneous. Obviously, for this to be valid, both types of elements must have equivalent stiffnesses. This has been shown to be true at the macro-level where both models predicted nearly identical material properties [6]. This approach also assumes that the boundary displacements predicted by the homogeneous element are not significantly different from those that would occur if a heterogeneous medium was accurately modeled. By using displacement boundary conditions, rather than stress boundary conditions, any errors introduced by this approach should be minimal.

The objective of this paper is to demonstrate the viability of this approach to a macro-micro analysis and to present results for a unidirectional

boron/aluminum monolayer with a center notch. This paper will first present a brief description of the macro- and micro-level finite element programs. Next, the procedure used to link the macro-level and DFM models is described. Then, stress components within the DFM model were calculated and stress distributions are presented along selected planes and surfaces within the DFM model, including the fiber-matrix interface. Finally, yielding in the matrix is examined near the notch tip.

SPECIMEN AND GEOMETRY

The composite specimen modeled in the analyses was a boron/aluminum (B/Al) monolayer made by diffusion-bonding a sheet of 0.142-mm-diameter boron fibers between two 6061 aluminum foils. The monolayer was 0.279 mm thick with a fiber volume fraction of 0.30. The material was used in the as-fabricated condition; that is, it was not heat treated. The monolayer specimen, as shown in Figure 1, was 78 mm wide (2W), 101 mm long (2H), with a center crack-like notch 19 mm long (2a) and 0.127 mm wide. The nonlinear behavior of the matrix material was fit with a Ramberg-Osgood equation, where the modulus of the aluminum was 72340 MPa, Poisson's ratio was 0.30, and the proportional limit was 34.5 MPa. The fiber was assumed to be a homogenous, isotropic material with a modulus of 400000 MPa and a Poisson's ratio of 0.13 [1]. Testing of this specimen is described in [1].

ANALYTICAL MODELING

Macro-Level Analysis

The macro-level analysis was conducted with a three-dimensional finite element program called PAFAC [7], which was developed from a program written by Bahei-El-Din et al. [8,9]. PAFAC uses a constant strain, eight-noded, hexahedral element. Each hexahedral element represents a unidirectional composite material whose fibers can be oriented in the appropriate direction in the structural (Cartesian) coordinate system. The PAFAC program uses the vanishing-fiber-diameter (VFD) material model developed by Bahei-El-Din and Dvorak [8, 10, 11] to model the elastic-plastic matrix and elastic fiber. The Ramberg-Osgood equation was used to model the nonlinear stress-strain curve of the aluminum matrix. The fiber was modeled as an linear, elastic material. The PAFAC program predicts fiber and matrix stresses at each element centroid.

The finite element mesh used to model the center-notched monolayer is shown in Figure 2. Only one-eighth of the specimen was modeled because of symmetry. The macro-level mesh is defined with respect to the global X-, Y-, and Z-axes as indicated in Figure 2. This mesh used 1389 nodes and 800 elements. As shown in Figure 1, a uniform stress in the Z-direction was applied to the end of the specimen to simulate tensile loading. The notch-tip element that was modeled by the micro-analysis is indicated in Figure 2 by the shaded element. The macro-analysis predicted the maximum fiber axial stress in the element at this location.

In the macro-analysis, further mesh refinement could have been used. However, for an individual element to have any physical meaning, the smallest size possible is that of a single fiber and its surrounding matrix. Thus, the notch-tip element was sized to represent one fiber and the surrounding matrix.

The dimensions of this element were calculated based on the fiber diameter, monolayer thickness, and fiber volume fraction of the composite. The rectangular mesh pattern shown in Figure 2 was chosen to best model the longitudinal shear yielding at the notch tip in unidirectional laminates [12].

Discrete Fiber-Matrix Model

Figure 3 shows how the DFM model was defined with respect to the macro-level mesh and where it is located with respect to the notch tip. Because of symmetry, one half of the fiber and the surrounding matrix were modeled. Figure 4 shows the dimensions of the discrete fiber-matrix (DFM) model; the DFM model has the same dimensions as the notch-tip element in the macro-level analysis. Figure 4 shows the finite element mesh that was used in the DFM model. The DFM mesh is defined with respect to the local x-, y-, and z-axes as indicated in Figure 4. A convergence study was performed to determine the mesh refinement by examining the radial and tangential stresses along the fiber-matrix interface for various mesh refinements. Eight layers of elements were used in the fiber or z-direction. The MSC/NASTRAN finite element code was used in the DFM analysis with eight-noded, isoparametric, hexahedral elements. A piece-wise linear approximation of the Ramberg-Osgood equation was used in NASTRAN to model the nonlinear stress-strain curve of the aluminum. The fiber was modeled as a linear, elastic material.

Determination of DFM Boundary Conditions

As mentioned earlier, the boundary conditions applied to the DFM model were determined from the macro-level finite element analysis. Displacement boundary conditions were used. The displacements of the element at the notch tip were used to calculate the boundary conditions to be applied to the DFM

model. The displacements for the corner nodes in the DFM model were taken directly from the macro-level analysis. To determine the displacements for the nodes on all the surfaces of the DFM model, second order Langrangian interpolation was used assuming that the nodal displacements from the macro-level analysis were a bivariate function. The displacements in the thickness or y-direction were assumed to vary linearly.

Due to symmetry in the macro-level model, the y-displacements on the local $y = 0$ face and the z-displacements on the $z = 0.0318$ mm face were constrained to be zero. To illustrate the calculation of the other boundary conditions, consider the geometry defined in Figure 5. The element drawn in solid lines is the element at the notch tip modeled by the DFM model. The elements drawn in dashed lines are the adjacent 3D elements in the macro-level analysis. The displacements from adjacent nodes were used to determine the appropriate boundary conditions as follows. Consider, for example, the face of the DFM model in the xz-plane defined by the node points 6, 8, 16, and 14 in Figure 5. The displacements on the larger surface in xz-plane defined by nodes 2, 8, 32, and 26 were fit to a bivariate function using a second order polynomial to determine an equation for the displacements of this surface. The displacements of all 16 nodes on this surface were used to determine this surface equations. The coordinates of all nodes on this face in the DFM model were then used with this equation to calculate the displacements of the boundary nodes of the DFM model. Since the macro-analysis model had only one layer of elements in the y-direction, macro-level nodal displacements are available for only two node points, a linear displacement distribution was assumed through the thickness.

A set of displacement boundary conditions were determined for the element location in the macro-level model shown in Figure 3, the element next to the notch tip.

RESULTS AND DISCUSSION

In all cases, results are presented for element centroidal stresses. Stress contours for the fiber and matrix, and plots of the interface stresses are presented for a unit applied remote stress. Stresses are presented with respect to the cylindrical coordinate system defined in Figure 4. Yielding predicted by the DFM analysis is also presented.

Matrix Stresses

Stress contours are presented for an elastic stress state due to a remotely applied unit stress (S = 1.0 MPa in Figure 1). Figures 6, 7, and 8 show predicted stress contours for the z = 0.0318 mm face of the DFM model. The notch tip is located on the right side of this face in the DFM model in the following figures. These figure show the matrix only in the DFM model. For clarity, fiber stresses will be shown separately in a following section.

Figure 6 presents the σ_{rr} stress contours in the matrix. The highest σ_{rr} stresses are on the side of the fiber away from the notch tip at $\theta = 180°$ due to the constraint provided by the adjacent fiber. However, the stresses next to the notch ($\theta = 0°$) are nearly as large as at $\theta = 180°$. Some small compressive stresses are present next to the fiber-matrix interface near $\theta = 100°$.

Figure 7 presents the $\sigma_{\theta\theta}$ stress contours in the matrix. These stresses are of approximately the same magnitude as the σ_{rr} stresses. The maximum $\sigma_{\theta\theta}$

stresses occur at the free surface at the upper corner next to the notch tip. The $\sigma_{\theta\theta}$ stresses around the fiber are greatest on the side of the fiber next to the notch tip.

Figure 8 presents the σ_{zz} stress contours in the matrix. This is the stress component in the fiber axial and loading direction; thus, these stresses are of the largest magnitude. As expected, the largest σ_{zz} stresses occur at the free surface next to the notch tip near $\theta = 0°$ and predict a matrix stress concentration factor greater than 7. The macro-analysis predicted a matrix stress concentration factor of 11 for the remote unit stress. In the DFM model, the σ_{zz} stresses increase fairly uniformly across the width with increasing distance from the notch. A second stress concentration occurs at $\theta = 180°$ due to the constraint provided by the adjacent fiber.

The $\tau_{r\theta}$ stresses are of particular interest at the fiber-matrix interface; thus, this stress component is discussed in the next section. Due to symmetry, the τ_{rz} and $\tau_{\theta z}$ are zero on the XY-plane (z = 0.318-mm face); stress contours are not shown for these components.

Interface Stresses

Since material properties for the interface between the fiber and the matrix are not known, the interface region was not modeled as a discrete region with distinct properties, only fiber and matrix were modeled. Interface stresses were calculated in the layer of matrix elements next to the fiber. Interface stresses are presented with respect to the cylindrical coordinate system shown in Figure 4, where $\theta = 0°$ is the side of the fiber closest to the notch tip. Interface stresses are shown for an elastic stress state due to a remotely applied unit stress (S = 1.0 MPa in Figure 1).

Figure 9 presents a polar plot of the interface stresses due to a remote unit stress. The σ_{rr} stresses (solid curve) have a maximum tensile value at $\theta = 0°$ and 180°, with the slightly larger stress at $\theta = 0°$, next to the notch tip. The σ_{rr} stress has a compressive peak at $\theta = 85°$. Due to the σ_{rr} component, the matrix wants to pull away from the fiber along the specimen mid-plane, while compressing the fiber near $\theta = 90°$.

Due to symmetry, $\tau_{r\theta}$ (dashed curve) is zero at $\theta = 0°$ and 180°. The maximum values of $\tau_{r\theta}$ occur near $\theta = 140°$ (negative shear stress) and $\theta = 50°$ (positive shear stress).

In general, the τ_{zr} shear stress should be considered as an interface stress. However, in this case, due to symmetry, this stress component is zero on the z = 0.0318-mm face of the DFM model.

Figure 9 also shows the $\sigma_{\theta\theta}$ stress at the interface (dash-dot curve). While this stress component is not usually considered an interface stress, since it does not act in the plane of the interface, it is an important component to consider in determining fiber-matrix separation. A tensile or positive $\sigma_{\theta\theta}$ stress will cause the matrix to grip the fiber, even if the interface has completely failed. This behavior was observed experimentally for Ti-15-3/SCS_6 composites [13]. Figure 9 shows that, for the notch-tip element, the $\sigma_{\theta\theta}$ is tensile for all values of θ and reaches a maximum value at $\theta = 0°$.

Along the specimen midplane ($\theta = 0°$ and 180°), the σ_{rr} stress would cause the matrix to pull away from the fiber, despite the tensile $\sigma_{\theta\theta}$ stresses which generally cause the matrix to grip the fiber. If the σ_{rr} governs failure of the interface, the most likely location for failure is at $\theta = 0°$. Normal and shear components vary around the fiber, suggesting that a multi-axial stress criterion may be required to predict interfacial failure and fiber-matrix

separation. One caution should be noted. This analysis does not account for thermal residual stresses. Predictions of the stress state at the interface can be significantly altered by including thermal residual stresses [13].

Fiber Stresses

The fiber stresses are presented for an elastic stress state due to a remotely applied unit stress (S = 1.0 MPa in Figure 1). Figures 10, 11, and 12 show predicted stress contours for the z = 0.0318 mm face of the DFM model. For clarity, only the fiber is shown in these figures. The notch tip is located to the right side of the fiber in these figures.

Figures 10 and 11 show the σ_{rr} and $\sigma_{\theta\theta}$ stress contours, respectively, for the fiber. Figure 10 shows that the σ_{rr} stresses are compressive through most of the fiber, becoming tensile on the side of the fiber away from the crack. The largest magnitude σ_{rr} stresses occur at θ = 90° near the fiber centroid. The $\sigma_{\theta\theta}$ stresses, shown in Figure 11, are entirely compressive with the largest magnitude near θ = 90°.

The macro-level analysis calculated the σ_{zz} stress in the fiber in the notch-tip element to be 25 MPa for a remote unit applied stress. Figure 12 presents the σ_{zz} stress contours in the fiber for the remote unit stress. As expected, the σ_{zz} stresses are largest on the side of the fiber next to the notch tip. The maximum point value of the σ_{zz} stress is 32 MPa at θ = 0° with an average σ_{zz} stress of 22 MPa, compared to 25 MPa predicted by the macro-analysis. Similar differences between the DFM and macro-analysis predictions were found for the other fiber stress components. This is expected since the DFM analysis calculates a varying stress distribution through the cross-section, where the macro-analysis only calculates a single value for each stress component. Thus, the two analyses agree very well for average values,

but a homogeneous model such as the VFD can not model such detailed behavior as is possible with the DFM analysis.

Yielding

Based on the von Mises yield criterion, the macro-level analysis predicted yielding of the notch-tip element at an applied remote stress of 8 MPa. A nonlinear analysis using the DFM model was done for the displacement boundary conditions corresponding to this remote stress. Figure 13 shows the von Mises equivalent stress contours for S = 8 MPa, where the von Mises equivalent stress, $\bar{\sigma}_{vm}$, is defined as follows:

$$\bar{\sigma}_{vm} = \sqrt{\sigma_x^2 + \sigma_y^2 + \sigma_z^2 - \sigma_x\sigma_y - \sigma_y\sigma_z - \sigma_z\sigma_x + 3(\tau_{xy}^2 + \tau_{yz}^2 + \tau_{zx}^2)}$$

When the von Mises equivalent stress is greater than or equal to the proportional limit ($\bar{\sigma}_{vm} \geq 34.5$ MPa), the matrix elements within the DFM mesh have yielded. Thus, in Figure 13, the area to the right of contour line A has yielded; approximately one third of the DFM model has yielded at the remote stress of 8.0 MPa. The macro-analysis predicted the entire element to be yielded at this stress level.

The DFM analysis predicted that yielding initiated next to the notch tip at an applied remote stress of 5.75 MPa, 28% lower value than the stress level of 8.0 MPa predicted by the macro-level analysis. As with the stress predictions, this difference is not unexpected. The finer mesh used in the micro-analysis results in predictions of steeper stress gradients and higher peak stresses, which leads to predictions of lower remote stresses to yield the matrix. Both analyses agreed well when predicting the unnotched laminate stress-strain curve.

All the displacement boundary conditions calculated from the macro-analysis are for an elastic stress state. As mentioned earlier, these displacement boundary conditions will be valid only if any yielding in the DFM model is limited to a small region. Large scale yielding in the DFM model would affect the displacements of the boundary nodes; thus, the displacements predicted by the macro-level analysis assuming that the notch-tip element is behaving elastically would no longer be valid. Figure 11 shows that the yielding is indeed small-scale; therefore, the displacement boundary conditions from the macro-analysis are valid.

Figure 14 shows a plot of the von Mises equivalent stresses in the fiber for the remote stress S = 8.0 MPa. Since the fiber is assumed to behave elastically, these stresses have no meaning in relation to a yield criterion. However, this equivalent stress can be viewed in terms of a failure criterion for the fiber. The maximum equivalent stress is predicted at the edge of the fiber next to the notch tip. Since the matrix and the interface in this region are also highly stressed, this area would be a likely location for crack initiation and interface failure. In this particular case, due to symmetry, the equivalent fiber stresses for the notch tip element are very similar to the fiber σ_{zz} stresses shown in Figure 12, thus, σ_{zz} alone could be used to predict fiber failures. However, in general, all stress components should be considered for a fiber failure criterion. Earlier work with notched B/Al laminates [1] used a two-parameter failure criterion based on axial and shear stress in the fiber to accurately predict the first fiber failure.

CONCLUDING REMARKS

A macro-micromechanics analysis was formulated to determine the matrix and fiber behavior near the notch tip in a center-notched metal matrix composite. The viability of this approach is demonstrated and results are presented for a boron/aluminum monolayer. The macro-level analysis models the entire notched specimen using a three-dimensional homogeneous, orthotropic finite element program which uses the vanishing-fiber-diameter (VFD) model to compute the elastic-plastic behavior of the matrix and the elastic behavior of the fiber. The micro-behavior is analyzed using a discrete fiber-matrix (DFM) model containing one fiber and the surrounding matrix. The boundary conditions applied to the DFM model were determined from the macro-level analysis. The dimensions of the DFM model were determined by the ply thickness and the fiber volume fraction and corresponded to the size of the notch-tip element in the macro-level analysis. Stress components within the DFM model were calculated and stress distributions are presented along selected planes and surfaces within the DFM model, including the fiber-matrix interface.

The DFM model predicted significantly higher maximum stresses in the notch-tip matrix and fiber, where a very non-uniform stress state was present, compared to the macro-analysis, which assumes an average stress state in each element. In particular, the predictions of fiber axial stress differed by 24%. However, the two analyses agree very well when predicting gross behavior such as moduli or unnotched stress-strain behavior.

In the notch-tip element, the interface stresses had significant shear and normal components, indicating that a multi-axial stress criterion may be necessary to analyze and predict fiber-matrix interface failure and

separation. A micro-level analysis, such as the DFM model, is necessary to analyze and predict interfacial behavior.

The DFM analysis predicted that yielding initiated at the free surface next to the notch tip, and progressed rather uniformly through the notch-tip element in a direction away from the notch tip. The DFM analysis predicted the initiation of yielding at a much lower stress level than the macro-analysis (28% difference), but the macro-analysis predicted the notch-tip element to be completely yielded at a stress level where the DFM analysis predicted only partial yielding.

In order to accurately analyze and predict interface stresses or stress distributions through a fiber cross-section, a micro-level analysis is required. A global analysis, such as the VFD model, is accurate only for predicting behavior in an average sense. But when combined with a micro-analysis, such as the DFM model, the two analyses can provide a detailed understanding of the microdamage development in metal matrix composites.

REFERENCES

1. Johnson, W. S., Bigelow, C. A., and Bahei-El-Din, Y. A., "Experimental and Analytical Investigation of the Fracture Processes of Boron/ Aluminum Laminates Containing Notches," NASA TP-2187, National Aeronautics and Space Administration, Washington, DC, 1983.

2. Griffin, O. H., Jr., and Vidussoni, M. A., "Global/Local Finite Element Analysis of Composite Materials," Computer Aided Design in Composite Materials. Proceedings of the International Conference, Southampton, England, April 13-15, 1988, Southampton, England/Berlin and New York, Computational Mechanics Publications/Springer-Verlag, 1988, pp. 513-523.

3. Foye, R. L.: An Evaluation of Various Engineering Estimates of the Transverse Properties of Unidirectional Composites. Proceedings of the Tenth National SAMPE Symposium--Advanced Fibrous Reinforced Composites, November 1966.

4. Chamis, C. C. and Sullivan, T. L.: Theoretical and Experimental Investigation of the Nonlinear Behavior of Boron Aluminum Composites. NASA TM X-68-205, NASA Lewis Research Center, 1973.

5. Adams, D. F.: Inelastic Analysis of a Unidirectional Composite Subjected to Transverse Normal Loading. Journal of Composite Materials, Vol. 4, 1970, pp. 310-328.

6. Bigelow, C. A.; Johnson, W. S.; and Naik, R. A.: A Comparison of Various Micromechanics Models for Metal Matrix Composites. The Third Joint ASCE/ASME Mechanics Conference, La Jolla, CA. July 9-12, 1989.

7. Bigelow, C. A.; and Bahei-El-Din, Y. A.: Plastic and Failure Analysis of Composites (PAFAC). LAR-13183, COSMIC, University of Georgia, 1983.

8. Bahei-El-Din, Y. A.: Plastic Analysis of Metal-Matrix Composite Laminates. Ph.D. Dissertation, Duke University, 1979.

9. Bahei-El-Din, Y. A.; Dvorak, G. J.; and Utku, S.: Finite Element Analysis of Elastic-Plastic Fibrous Composite Structures. Computers and Structures, Vol. 13, No. 1-3, June 1981, pp. 321-330.

10. Bahei-El-Din, Y. A.; and Dvorak, G. J.: A Review of Plasticity Theory of Fibrous Composite Materials. Metal Matrix Composites: Testing, Analysis, and Failure Modes, ASTM STP 1032, W. S. Johnson, Ed., American Society for Testing and Materials, Philadelphia, 1989, pp. 103-129.

11. Dvorak, G. J.; and Bahei-El-Din, Y. A.: Plasticity Analysis of Fibrous Composites. Journal of Applied Mechanics, Vol. 49, 1982, pp. 327-335.

12. Bigelow, C. A.: Analysis of Notched Metal Matrix Composites Under Tension Loading. Metal Matrix Composites: Testing, Analysis, and

Failure Modes, ASTM 1032, W. S. Johnson, Editor, American Society for Testing and Materials, Philadelphia, 1989, pp. 130-147.

13. Johnson, W. S.; Lubowinski, S. J.; Highsmith, A. L.; Brewer, W. D.; and Hoogstraten, C. A.: Mechanical Characterization of SCS_6/Ti-15-3 Metal Matrix Composites at Room Temperature. NASP Technical Memorandum 1014, April 1988.

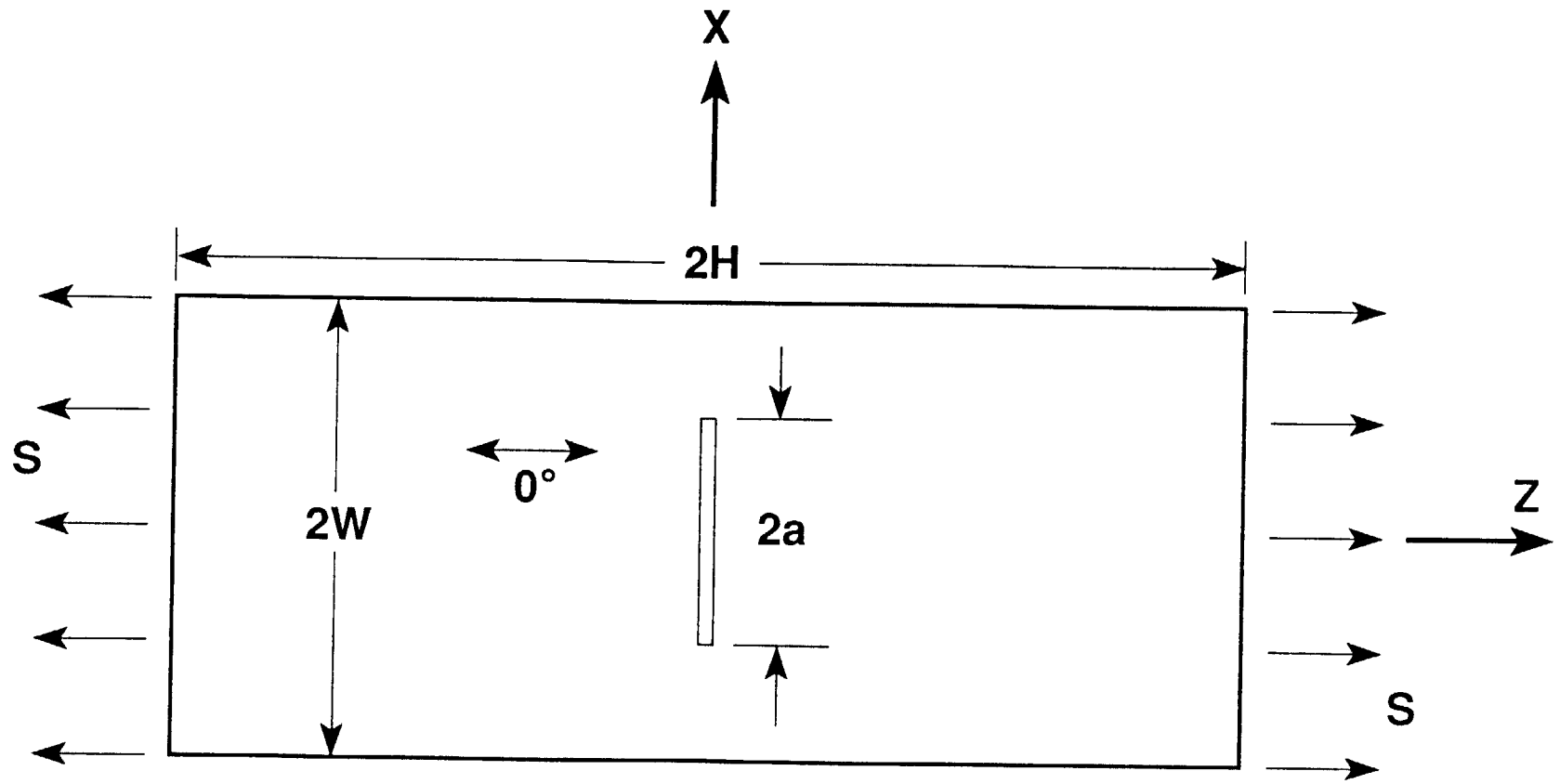

Figure 1. – Specimen geometry and loading. 2a = 19 mm, 2W = 78 mm, and 2H = 101 mm, v_f = 0.30.

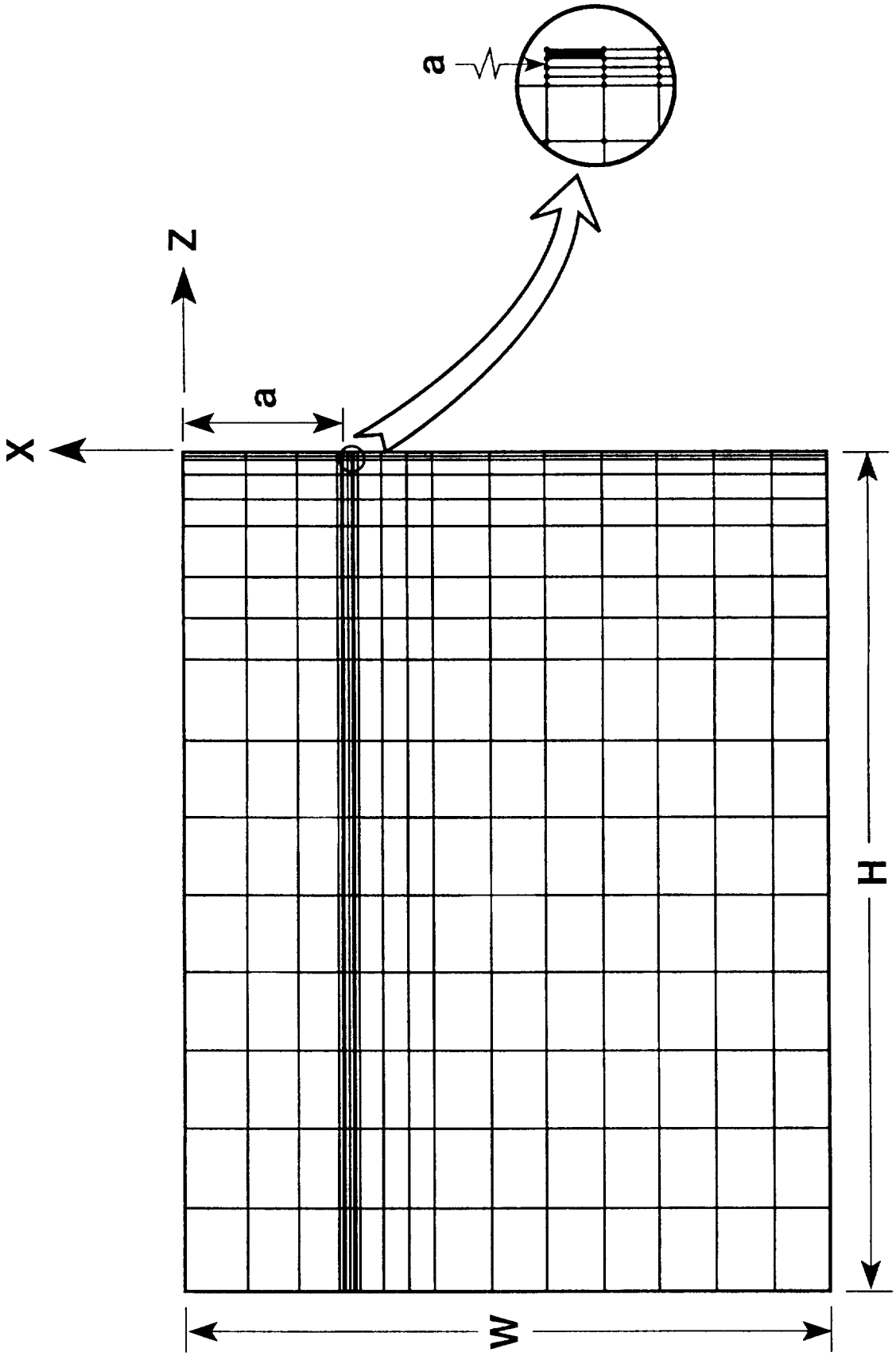

Figure 2. – Macro-level finite element mesh.

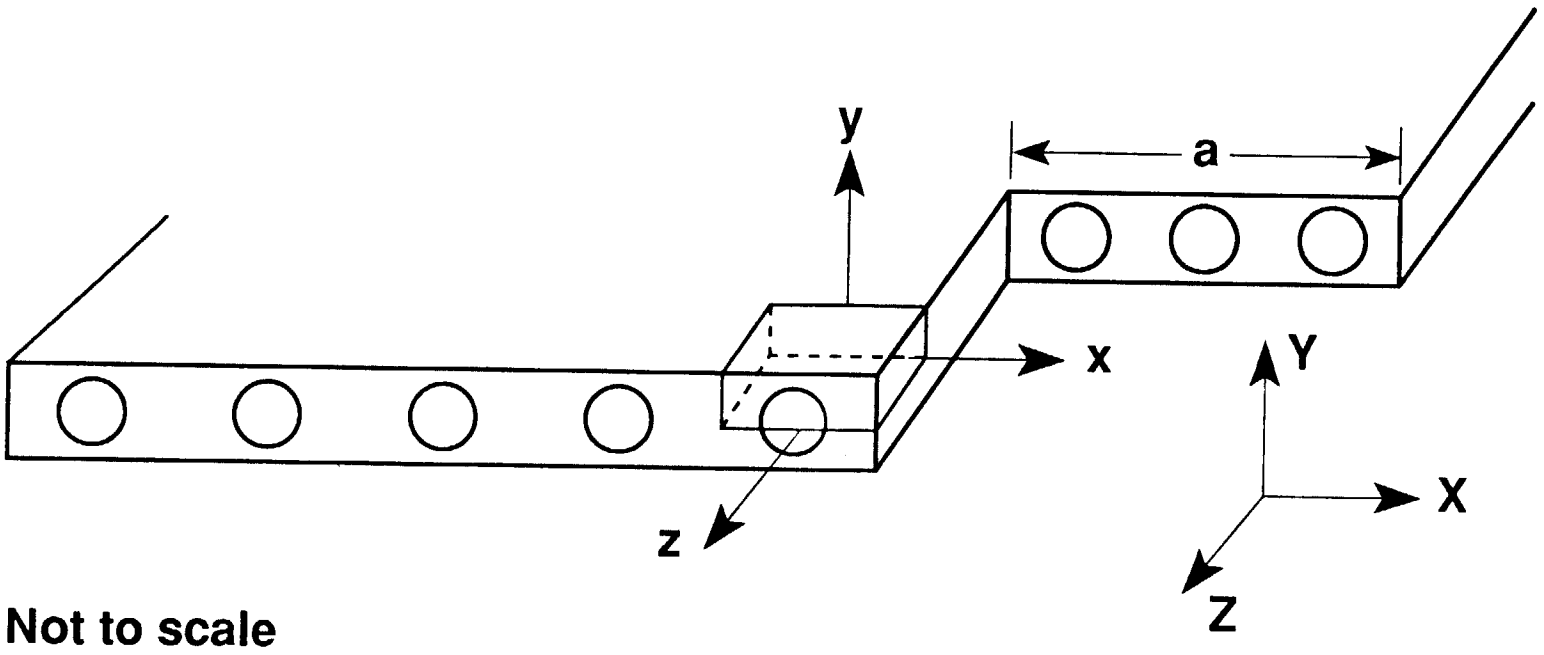

Figure 3. – Definition of micro– and macro–level models.

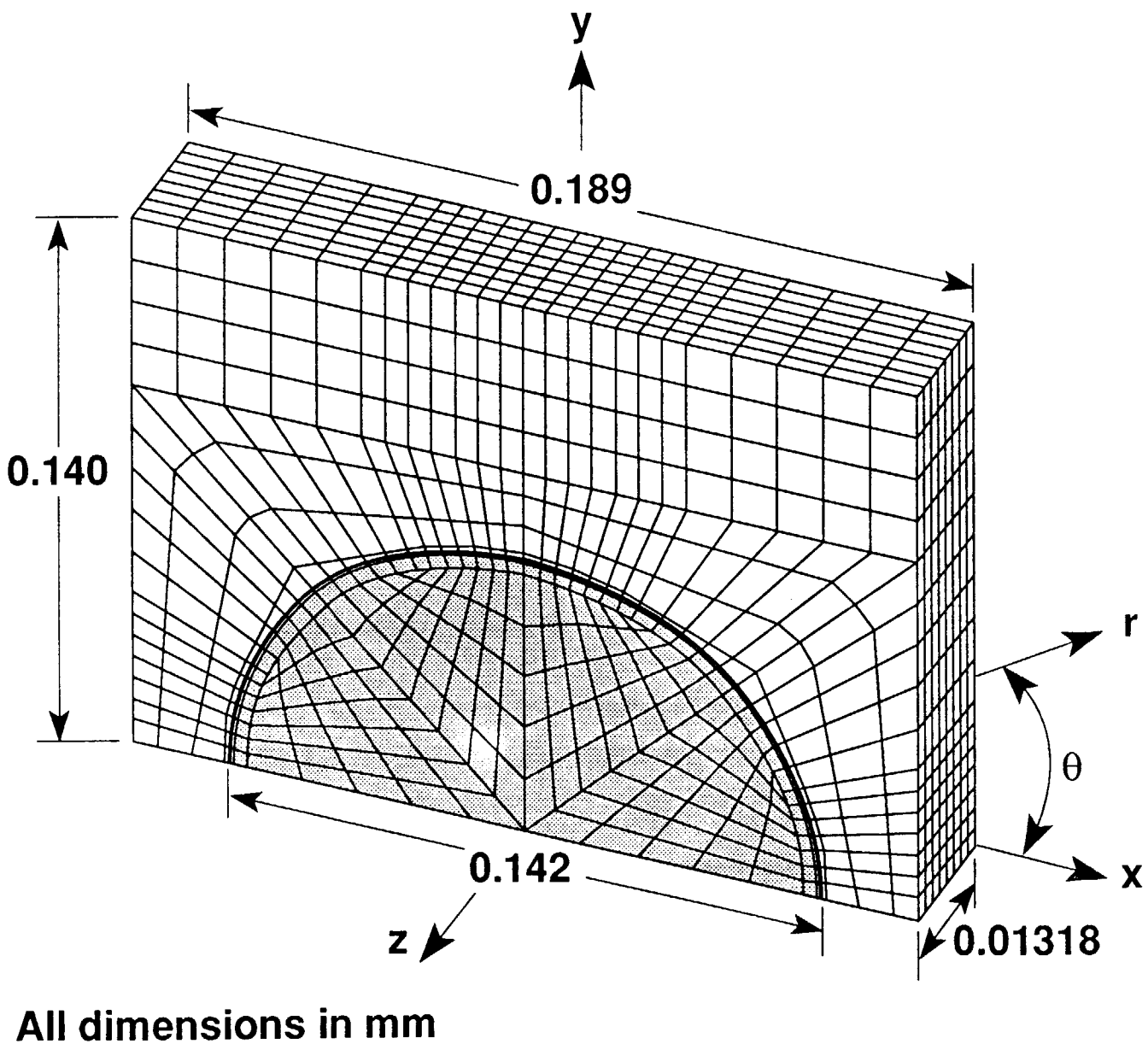

Figure 4. – Discrete Fiber–matrix (DFM) model.

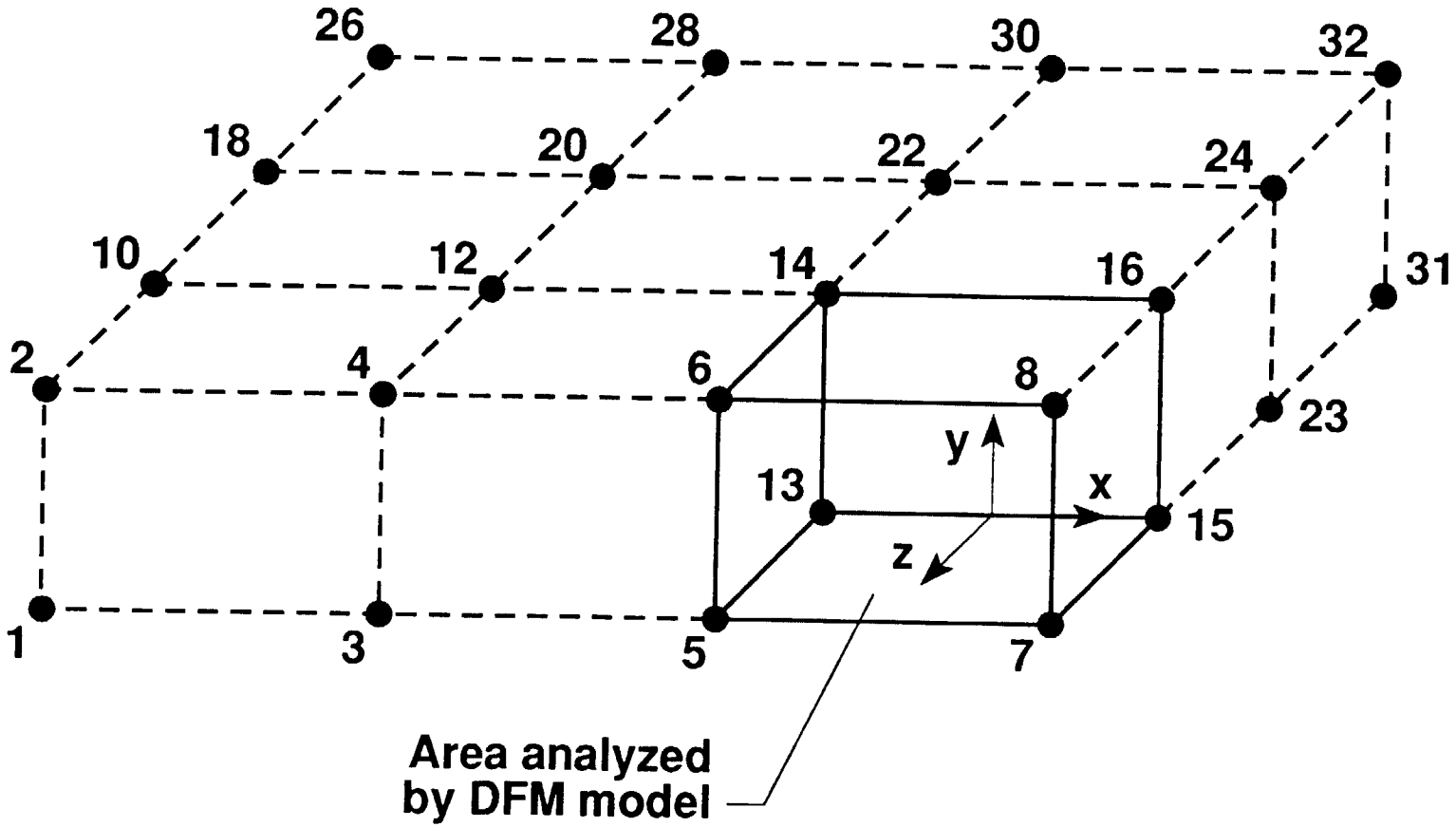

Figure 5. – Macro–level nodes used to define DFM boundary conditions.

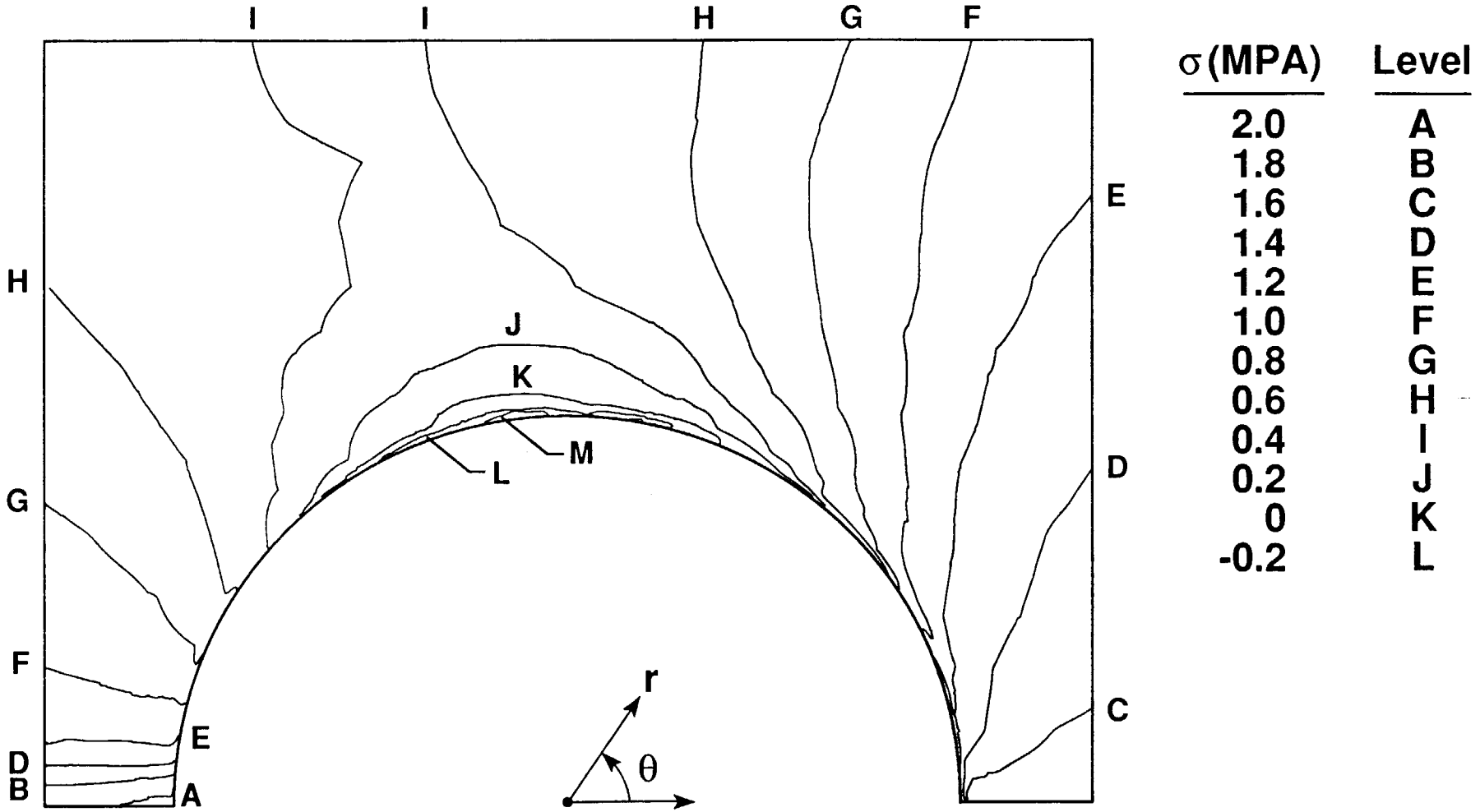

Figure 6. – Matrix σ_{rr} stress contours in notch–tip element for unit applied remote stress (S = 1.0 MPa)

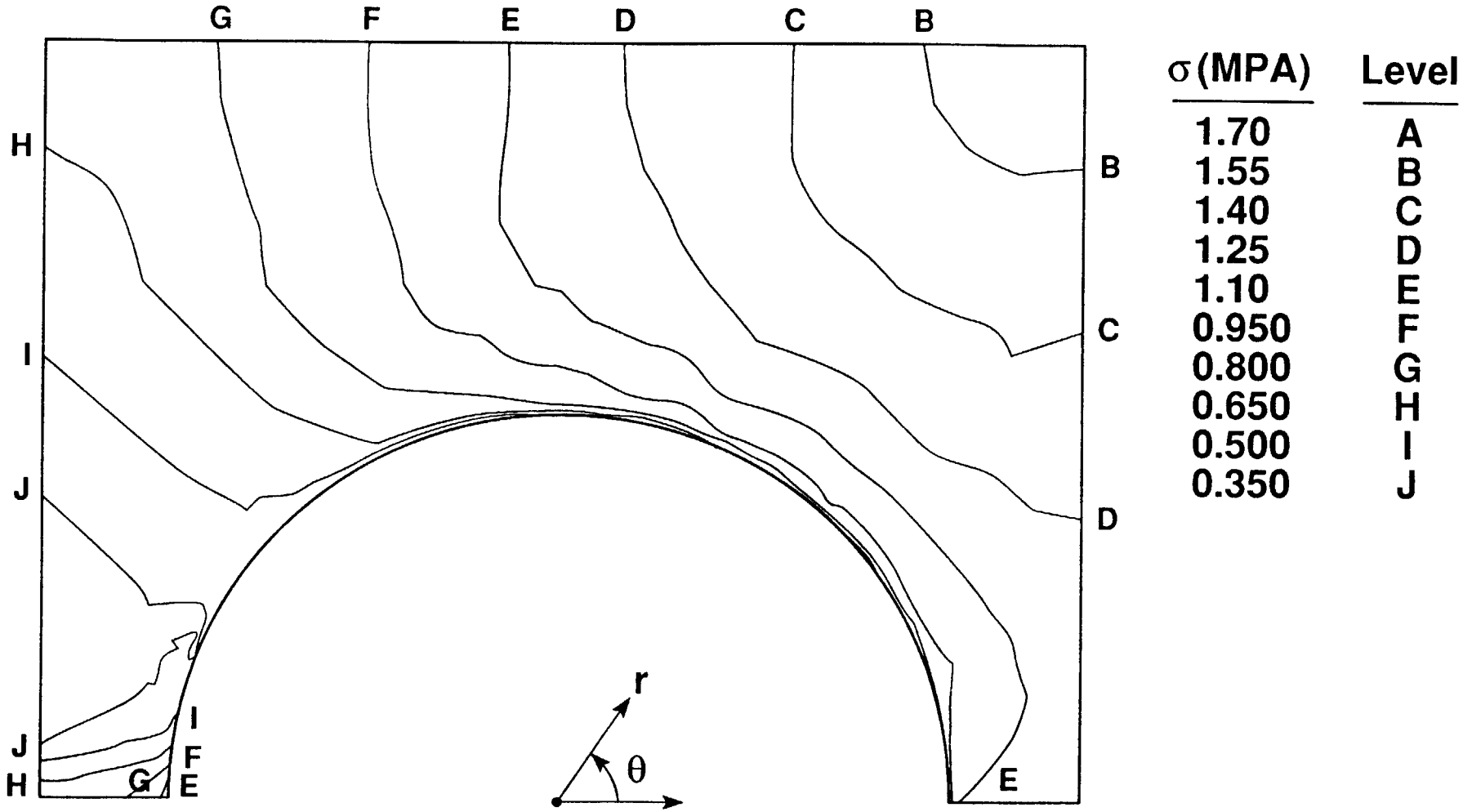

Figure 7. – Matrix $\sigma_{\theta\theta}$ stress contours in notch–tip element for unit applied remote stress (S = 1.0 MPa).

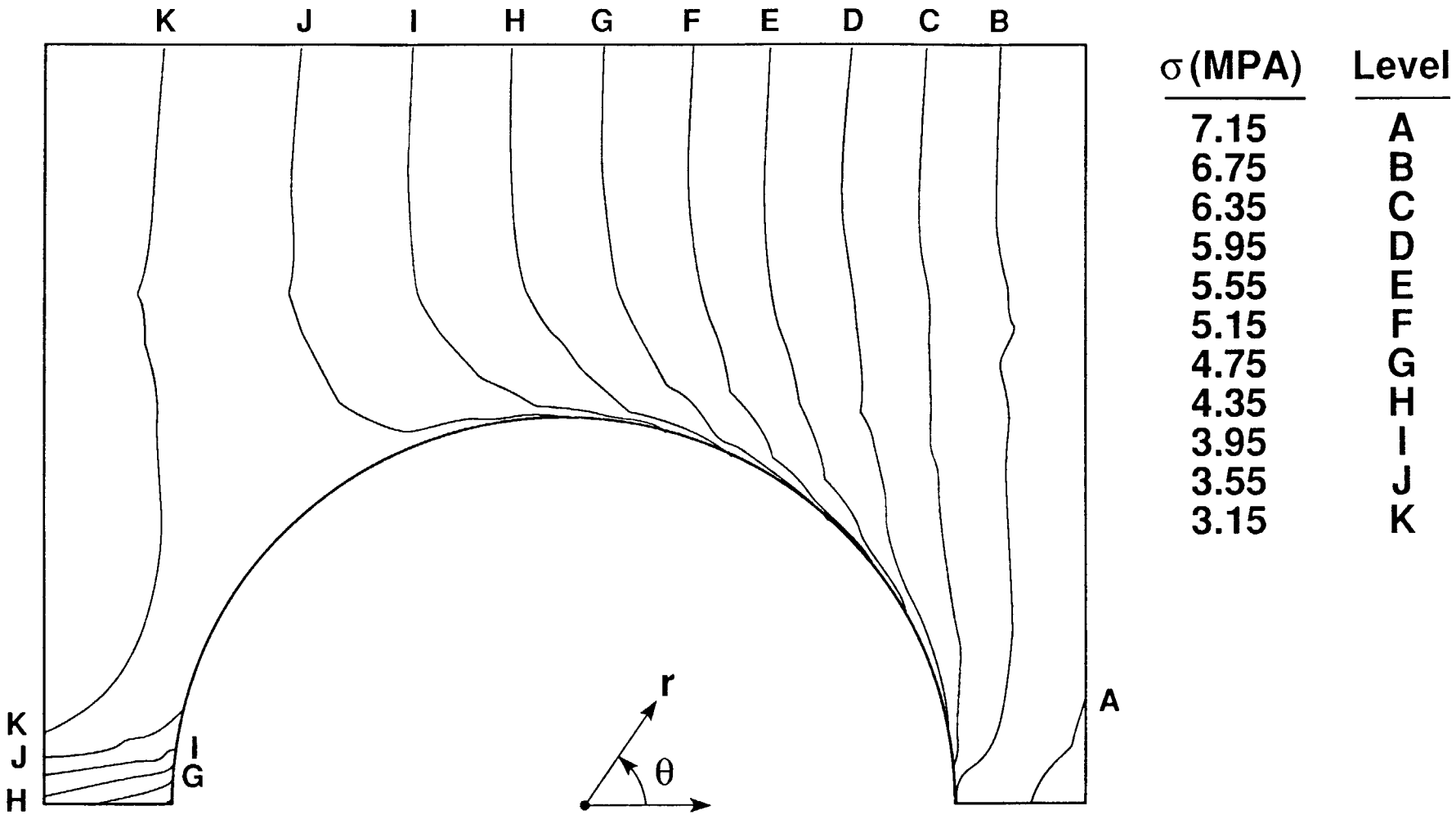

Figure 8. – Matrix σ_{zz} stress contours in notch–tip element for unit applied remote stress (S = 1.0 MPa).

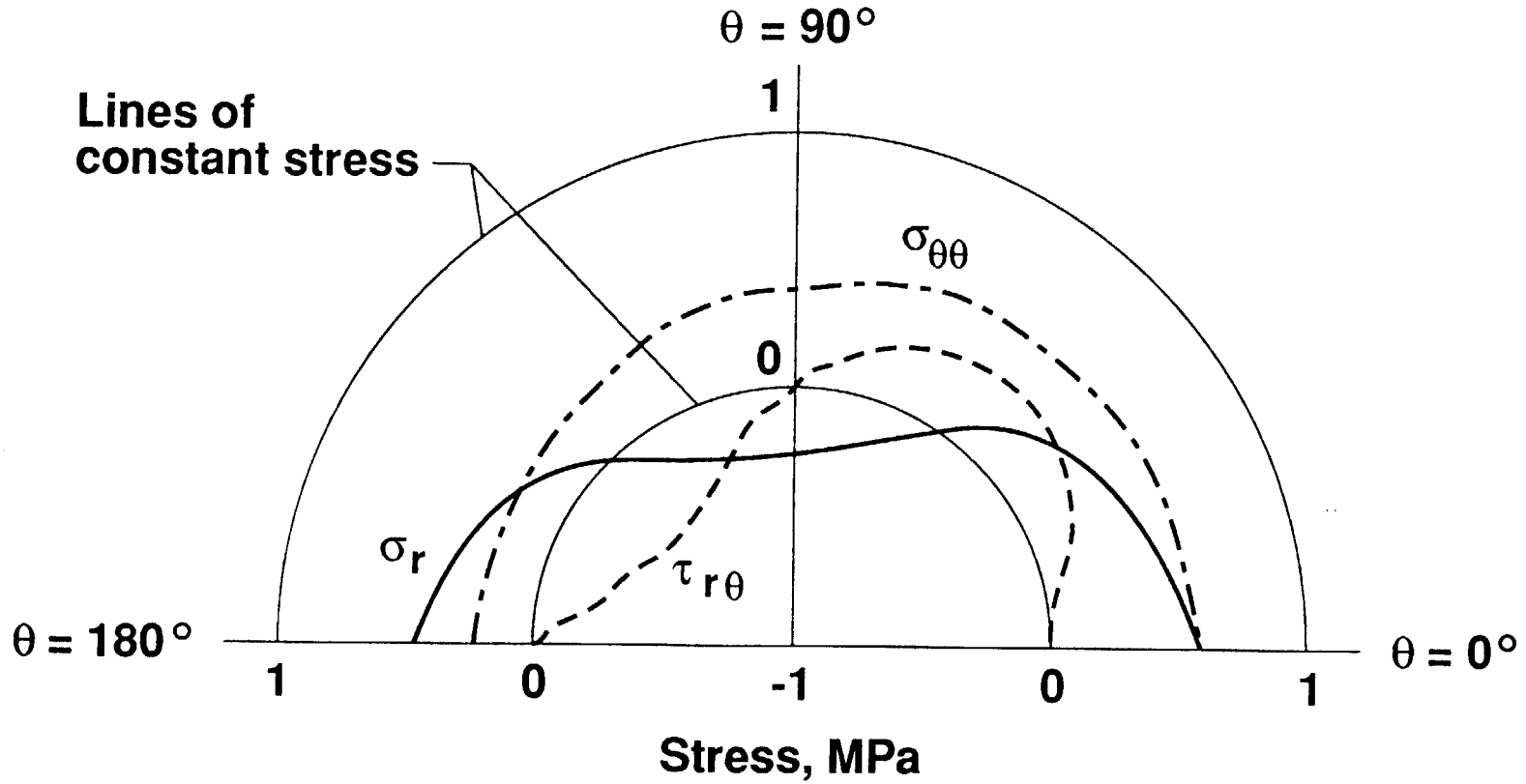

Figure 9. – Interface stresses for unit applied remote stress (S = 1.0 MPa).

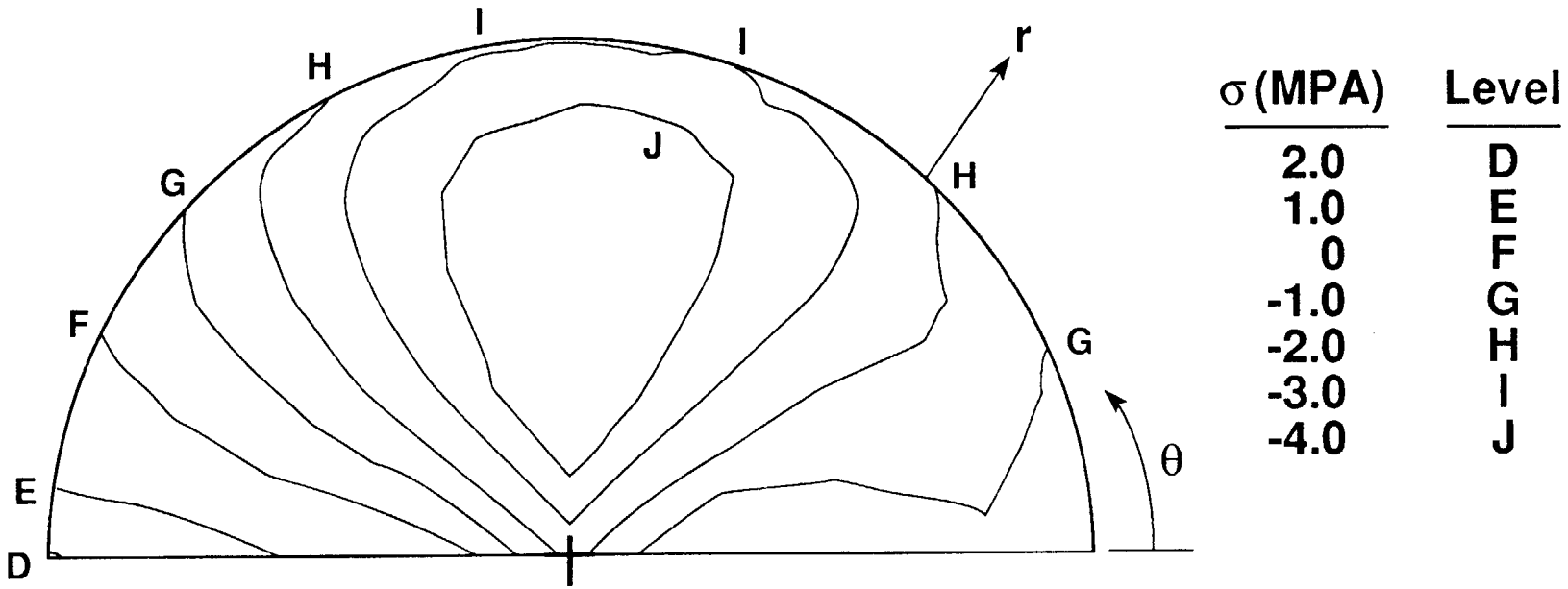

Figure 10. – Fiber σ_{rr} stress contours in notch–tip element for unit applied remote stress (S = 1.0 MPa).

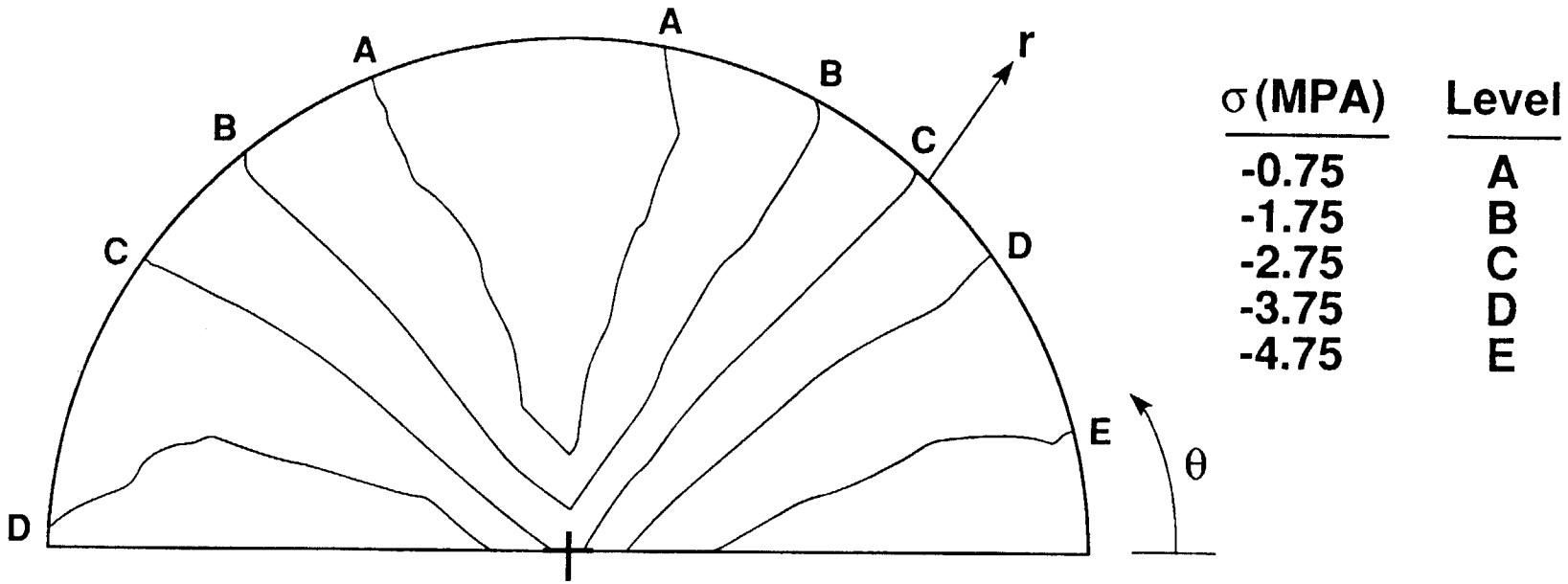

Figure 11. – Fiber $\sigma_{\theta\theta}$ stress contours in notch–tip element for unit applied remote stress (S = 1.0 MPa).

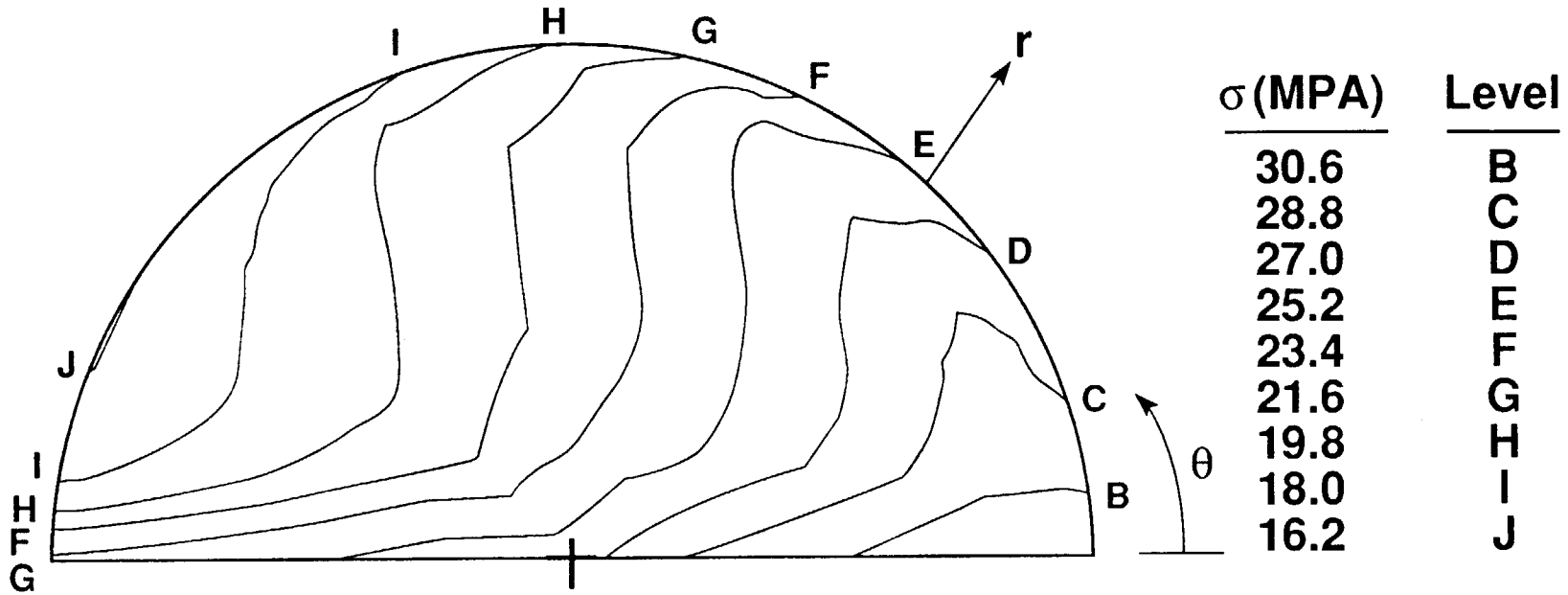

Figure 12. – Fiber σ_{zz} stress contours in notch–tip element for unit applied remote stress (S = 1.0 MPa).

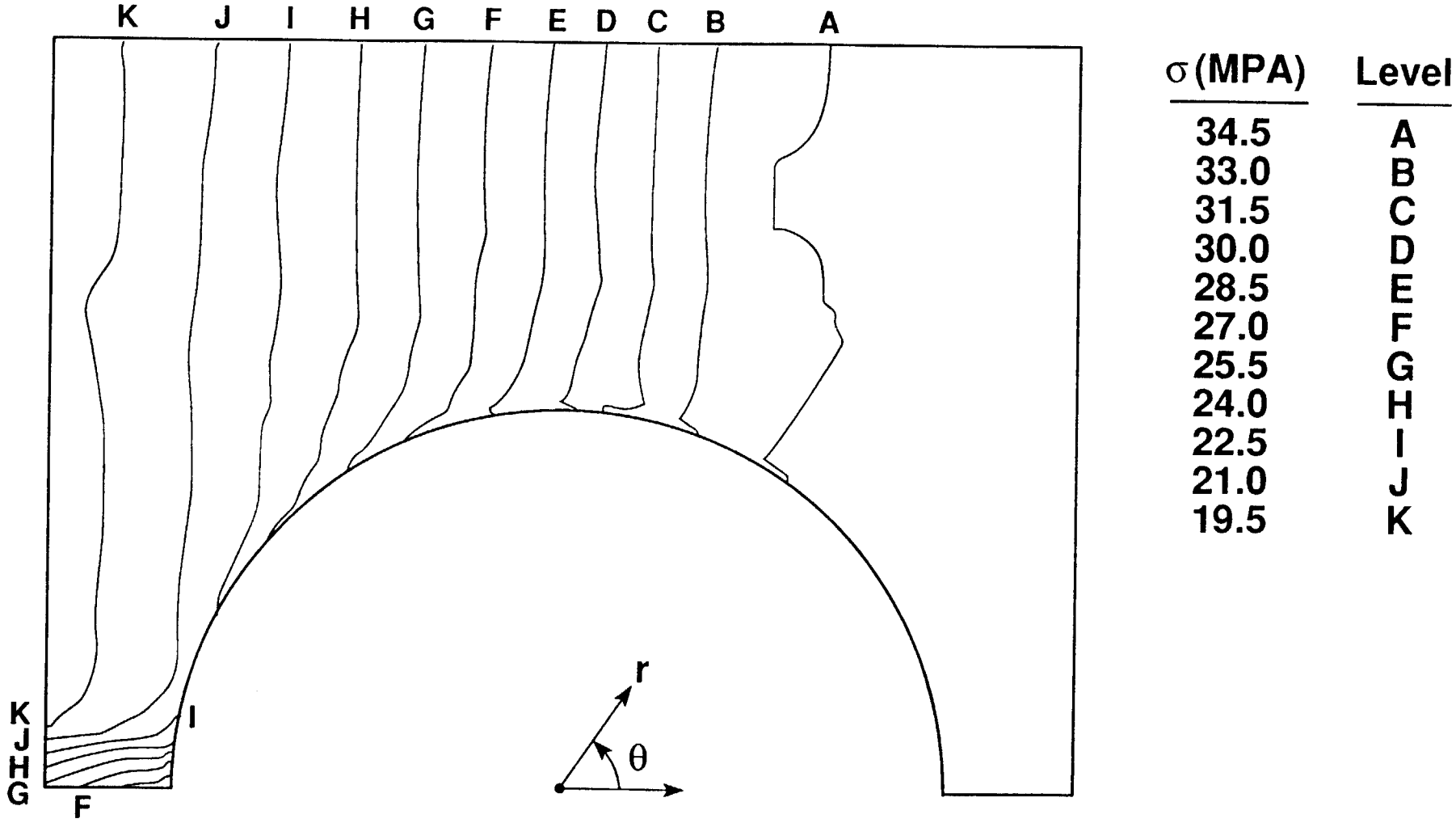

Figure 13. – Von Mises equivalent stress contours in matrix for applied remote stress, S = 8.0 MPa.

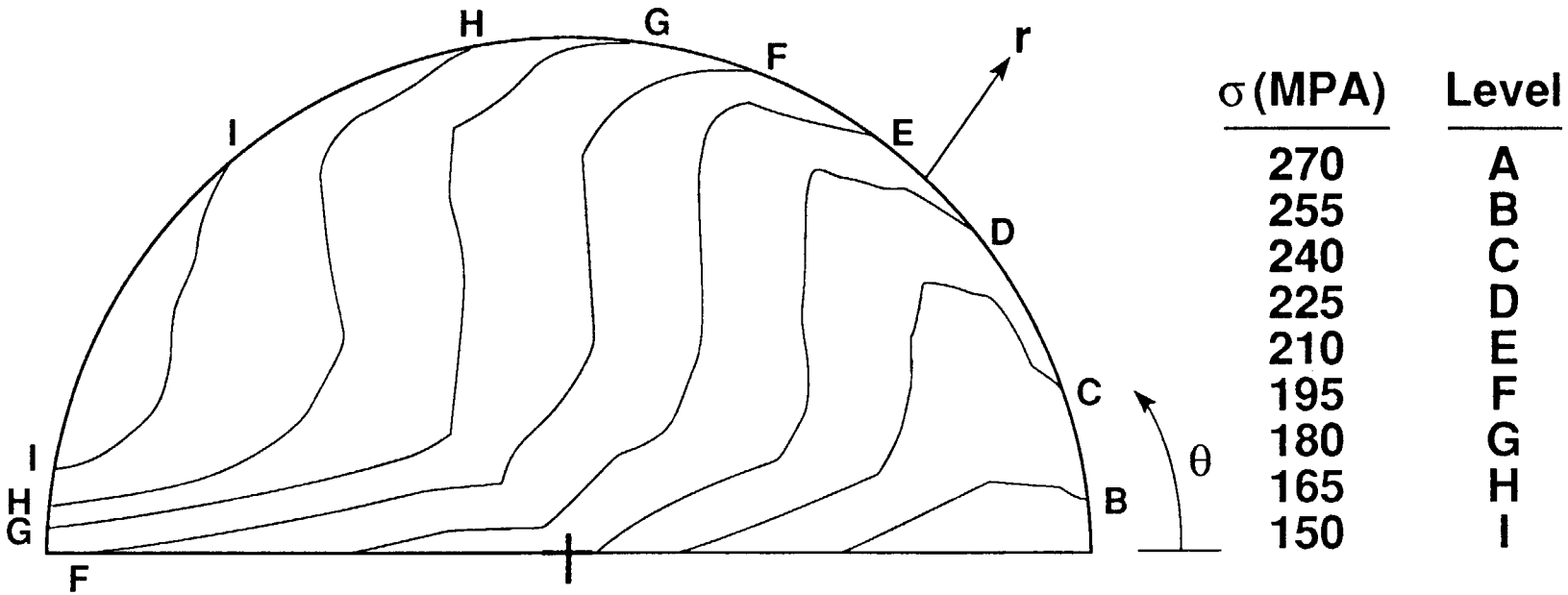

Figure 14. – Von Mises equivalent stress contours in fiber for applied remote stress, S = 8.0 MPa.

NASA

Report Documentation Page

1. Report No.	2. Government Accession No.	3. Recipient's Catalog No.
NASA TM-102728		

4. Title and Subtitle	5. Report Date
A Macro-Micromechanics Analysis of a Notched Metal Matrix Composite	September 1990
	6. Performing Organization Code

7. Author(s)	8. Performing Organization Report No.
C.A. Bigelow[1] and R. A. Naik[2]	
	10. Work Unit No. 505-63-01-05

9. Performing Organization Name and Address	11. Contract or Grant No.
NASA Langley Research Center, Hampton, VA 23665-5225	
	13. Type of Report and Period Covered Technical Memorandum

12. Sponsoring Agency Name and Address	14. Sponsoring Agency Code
National Aeronautics and Space Administration Washington, DC 20546-0001	

15. Supplementary Notes

[1]National Aeronautics and Space Administration, Hampton, VA
[2]Analytical Services and Materials, Inc., Hampton, VA

16. Abstract

A macro-micromechanics analysis was formulated to determine the matrix and fiber behavior near the notch tip in a center-notched metal matrix composite. Results are presented for a boron/aluminum monolayer. The macro-level analysis models the entire notched specimen using a three-dimensional finite-element program which uses the vanishing-fiber-diameter model to model the elastic-plastic behavior of the matrix and the elastic behavior of the fiber. The micro-behavior is analyzed using a discrete fiber-matrix (DFM) model containing one fiber and the surrounding matrix. The dimensions of the DFM model were determined by the ply thickness and the fiber volume fraction and corresponded to the size of the notch-tip element in the macro-level analysis. The boundary conditions applied to the DFM model were determined from the macro-level analysis. Stress components within the DFM model were calculated and stress distributions are presented along selected planes and surfaces within the DFM model, including the fiber-matrix interface. Yielding in the matrix was examined at the notch tip in both the macro- and micro-level analyses. The DFM model predicted higher stresses (24%) in the fiber compared to the global analysis. In the notch-tip element, the interface stresses indicated that a multi-axial stress criterion may be required to predict interfacial failure. The DFM analysis predicted yielding to initiate in the notch-tip element at a stress level 28% lower than predicted by the global analysis.

17. Key Words (Suggested by Author(s))	18. Distribution Statement
Boron/aluminum Global-local Elastic-plastic Interface Finite-element	Unclassified - Unlimited Subject Category - 24

19. Security Classif. (of this report)	20. Security Classif. (of this page)	21. No. of pages	22. Price
Unclassified	Unclassified	32	A03